

Dielectric Anisotropy of Human Bone and CERABONE® in the Terahertz Spectral Range 0.2 to 2.5 THz

A.S. Nikoghosyan¹, H. Ting², J. Shen², R.M. Martirosyan¹, M.A. Kazaryan⁴
M.Yu. Tunyan³, A.V. Papikyan³, A.A. Papikyan³

¹Yerevan State University, 1 Alex Manoogian, 0025 Yerevan, Armenia

²Capital Normal University, Key Laboratory for Terahertz Spectroscopy and Imaging,
Beijing, 100048 China

³Yerevan State Medical University, Yerevan, Armenia

⁴Optics, Lebedev Physical Institute, Moscow, Russia

E-mail: nika@ysu.am

Abstract.

Terahertz time-domain spectroscopy (THz-TDS) was applied to study properties of a human jawbone in transmission geometry. The fiber femtosecond laser (Fx-100, IMRA) with a pulse width of 113 fs, a central wavelength of 800 nm and an average power of 120 mW was used as a laser source for pumping and detecting terahertz pulses. The refractive indices $n(\omega)$ and absorption coefficients $\alpha(\omega)$ of the human jawbone and bone substitute Cerabone® were determined in vitro by the THz-TDS in a wide frequency range from 0.2 to 2.5 THz. It is shown that the refractive index of the human jawbone changes between the values of 2.24 and 2.36, and Cerabone® between 2.4 and 2.65. The absorption coefficient of the human jawbone depending on frequency increases from 1.7 cm^{-1} to 178.5 cm^{-1} , showing several resonance absorption lines after 1.6 THz. The absorption coefficient of Cerabone® increases from zero to 80 cm^{-1} , and the resonance absorption occurs at 1.7 THz. The experimental results indicate that $n(f)$ and $\alpha(f)$ of a human jawbone change with the alteration of the direction of the linear polarization vector of the electric field of THz pulse relative to the axis of the plate of the human jawbone. The obtained results allowed us to determine the proximity of the physical properties of the Cerabone® with the natural bone matrix.

PACS: <http://www.aip.org/pacs>

Keywords: terahertz time domain spectroscopy, dielectric anisotropy, human bone, terahertz range, Cerabone

1. Introduction

A bone material is composed of an organic matrix of collagen fibers and mineral hydroxyapatite ($\text{Ca}_5(\text{PO}_4)_3\text{OH}$) nanoparticles. An average tooth dentin contains 70% hydroxyapatite crystals, 20% collagen (e.g., proteins), and 10% water. The organic constituents provide flexibility, whereas the mineral provides strength and quality. Due to the specific arrangement of nanosized mineral platelets and collagen fibrils with respect to the main axis in case of a long bone (figure 1(a)), signals relative to vibrational units of both mineral and collagen can result highly anisotropic. Up to now, very few



Content from this work may be used under the terms of the [Creative Commons Attribution 3.0 licence](https://creativecommons.org/licenses/by/3.0/). Any further distribution of this work must maintain attribution to the author(s) and the title of the work, journal citation and DOI.

Published under licence by IOP Publishing Ltd

studies have been conducted concerning the study of the human bones [1,2] and its anisotropy by THz radiation [3].

Many biological tissues (eye cornea, retina, dura mater, teeth, tendon, cartilage, muscle, myocardium, artery wall, nerve, etc.) are structurally anisotropic. Tissue birefringence results from the linear anisotropy of fibrous structure. The refractive index of a medium is higher along the length of fibres than along their cross section [3]. A tissue structure is a system composed of parallel cylinders that create a uniaxial birefringent medium with the optic c-axis parallel to the fibrils (cylinders) axes, as shown in figure 1(b) [4, 5].

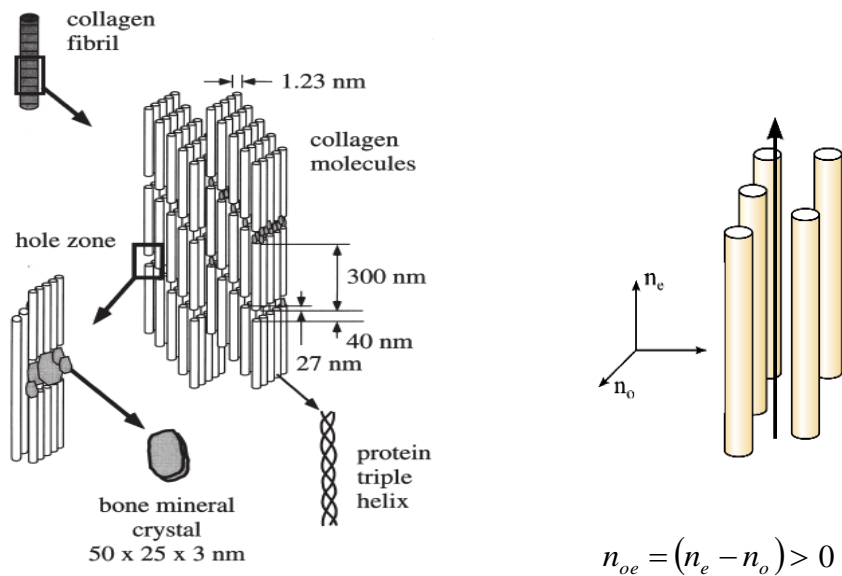


Figure 1. System of long dielectric cylinders array (mineralized collagen fibrils of turkey) with major components

A structure of parallel dielectric fibrils immersed in isotropic homogeneous ground substance behaves as a positive uniaxial birefringent medium $n_e - n_o > 0$, where n_e is the refractive index of extraordinary ray and n_o the refractive index of ordinary ray. The hidroxyapatite can be found in space between fibrils - in layers that transverse across the fibrils and both within and outside the collagen fibrils [6, 7]. The collagen fibrils periodically separated by a tiny gap from 1 nm to 67 nm. The results of electron diffraction and X-ray diffraction, carried out on samples, support the concept of organized intra-fibril mineral crystals within the organic collagen matrix.

THz wave (frequency range from 0.1 to 10 THz) found the most widespread practical use in THz time-domain spectroscopy [8,9] and in the THz imaging [10,11]. It is known that the time of vibrational motion of biological molecules have the order of picoseconds, and therefore, the frequency of vibrations is in the terahertz frequency range. Intermolecular interactions are usually weaker than the intramolecular and only THz spectroscopy in the time domain is sensitive to resolve their spectrum in the THz range. THz wave is non-invasive (since the photon energy of terahertz waves at several orders of magnitude smaller than the photon energy of the x-ray wavelength) and the non-contact nature, can penetrate into the non-conductive materials and to provide additional spectroscopic data for the accurate diagnosis and analysis of the material.

In this paper we report the results obtained from a study of dielectric anisotropic properties of a human jawbone in transmission geometry using THz time-domain spectroscopy (THz -TDS).

2. Experimental technique

A schematic arrangement of the THz-TDS system, demonstrating the principal configuration used to obtain THz spectral data, is shown in figure 2. The fiber femtosecond laser (Fx-100, IMRA) with a pulse duration of 112 fs, a central wavelength of 800 nm and an average power of 120 mW was used as a laser source for pumping and detecting terahertz pulses.

The laser output, in the form of high repetition frequency - 75 MHz, is divided into two optical paths - the pump and probe beams. The pump beam is focused into a gap between biased electrodes deposited upon the surface of gallium arsenide. The pumping pulses have photon energy (1.43 eV) above the direct band-gap of the GaAs this induced conductivity changes. Electron-hole pairs are created by each laser pulse in a semiconductor, which, when accelerated by the bias field, act as a transient current source. The transient current radiates a sub-picosecond, single-cycle coherent THz electric pulse, as shown in figure.3a. The THz pulse from photoconductive antenna (PCA) is emitted in a dipole like pattern. The resulting radiation is polarized along the direction of the bias field. The polarization ratio is usually better than 10:1.

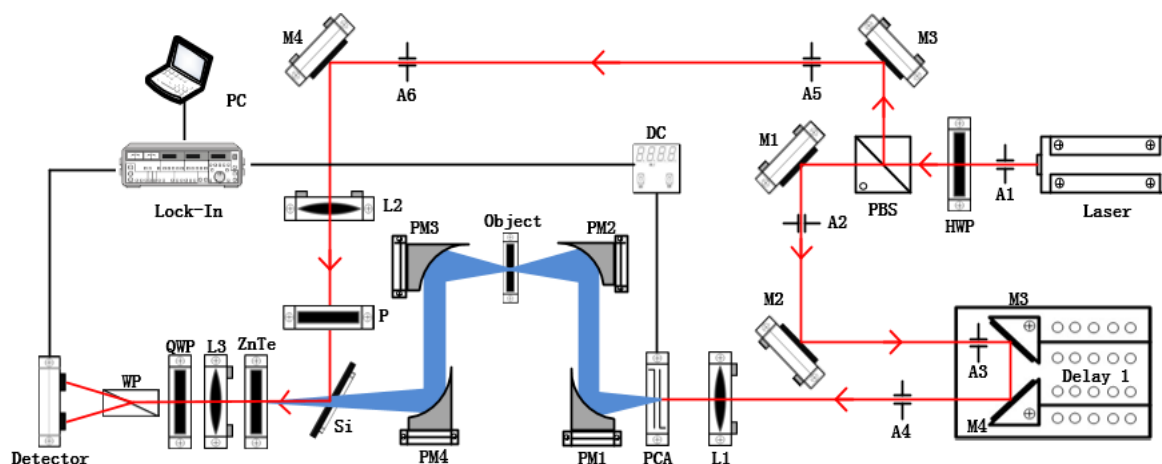


Figure 2. Experimental setup of the THz spectrometer.

Figure 2 is experimental setup of the THz spectrometer, where L is the femtosecond laser Fx-100, IMRA; A1–A6 the diaphragms; M1–M6 the mirrors deflecting the optical beam; DL optical delay line; PM1–PM4 the parabolic mirrors; HWP the half-wave ($\lambda/2$) plate; PBS the polarizing beam splitter; L1–L3 the focusing lenses; PCA the GaAs photoconductive antenna; DC the data acquisition software; P the polarizer; Si the silicon wafer which unites the THz and optical beams; ZnTe the crystal; QWP the quarter-wave ($\lambda/4$) plate; WP the Wollaston prism; S the test material; D the detecting diodes; LA the lock-in amplifier; PC the personal computer.

The THz pulse after PCA is collected and directed to the test material using parabolic mirrors PM1 and PM2. The THz radiation transmitted through the test material is then directed by two parabolic mirrors PM3 and PM4 towards a detector. The subpicosecond THz pulse and optical femtosecond pulse were combined by the thin plate of Si inside the ZnTe crystal.

A small fraction of the pump optical beam - probe beam, was used for coherent detection of transmitted radiation from the test material (jawbone) using a dynamic free-space electro-optic cell, which consists of an electro-optic crystal ZnTe with a (110) orientation and the thickness 1 mm, of the quarter-wave plate providing optical bias, and of the Wollaston prism (WP) as the analyzer. The probe

beam has controlled the detector, whose response was proportional to the amplitude and the sign of the electric field of the THz pulse. Thus, the whole system represents a version of a coherent pump-probe spectroscopic setup [12].

The electro-optic sampling method is widely applied for the coherent detection of THz pulse due to its short response time, high sensitivity and wide bandwidth. For the electro-optic sampling, the phase-matching condition requires the group velocity of probe pulse equal to the phase velocity of THz pulse. The phase mismatch is defined as [13]

$$\Delta k = \frac{f_{THz}}{c} (n_{THz}(f_{THz}) - n_g(f_{opt})) \quad (1)$$

The amplitude of detection response is proportional to the thickness of crystal ZnTe at the phase-matching condition, but a thicker crystal results in the reduction of bandwidth of THz pulse. The compromise should be made between the detection response and bandwidth. We used a ZnTe crystal of 1 mm thickness, ipso facto to provide the coherent detection of THz pulse in spectral range from 0.2 THz to 2.7 THz.

The temporal form of the THz pulse $E(t)$ was determined by the change in the time delay between pump and probe beams using the optical delay line (DL). The balanced electro-optic detection method provides an excellent signal to noise ratio >1500 (to a noise-limited frequency of 3 THz) by the use of phase sensitive amplification with a lock-in amplifier. The amplified signal from a lock-in amplifier is transmitted to the computer through the analog-to-digital converter. Two spectra, THz field $E(f)$ and phase $\Phi(f)$, are processed via a fast Fourier transform in the program Origin from originally obtained time-domain dependence $E(t)$.

3. Results and discussion

THz time-domain transmission spectroscopic properties of the jawbone is presented in figure 3 and figure 4. The temporal forms of the THz pulses transmitted through the air (reference pulse) and human jawbone and the corresponding THz field spectra obtained after the fast Fourier transform are shown in figures 3a,b,c. The phase-frequency dependences $\Phi_1(\omega)$ and $\Phi_2(\omega)$ are shown in figure 3d, and the refractive indices and absorption coefficients at figure 3e, f. The laser polarization is parallel to the bone axis. To demonstrate the reproducibility of the experiment, on figure 3 (b, c, e, f) the curves of three consecutive measurements are given. The thickness of the jawbone was 0.44 mm and the cross-section $2 \times 1 \text{ mm}^2$. During the measurements, the air temperature was 21°C , the humidity $< 1.5\%$, the dynamic range was more than 1000, and the signal/noise ratio at the peak position was about 400.

Temporal waveforms of THz pulses transmitted through the jawbone, THz amplitude spectra of the fields after a FFT, the index of refraction $n(\omega)$ and absorption coefficient $\alpha(f, \omega)$ for different directions of the laser polarization are depicted in figures 4 a-d. Figure 4(c) shows that the index of refraction $n(f)$ of the jawbone and therefore the velocity of the THz pulse is different for different directions of the THz polarization with respect to the axis of the plate of the human jawbone. The dispersion of the refractive index of jawbone is weak for all directions of polarization, however, $n_{45}(f)$ is greater than the value $n_{ver}(f)$ and $n_{par}(f)$ at any frequency in the spectral range of 0.2-1.5 THz.

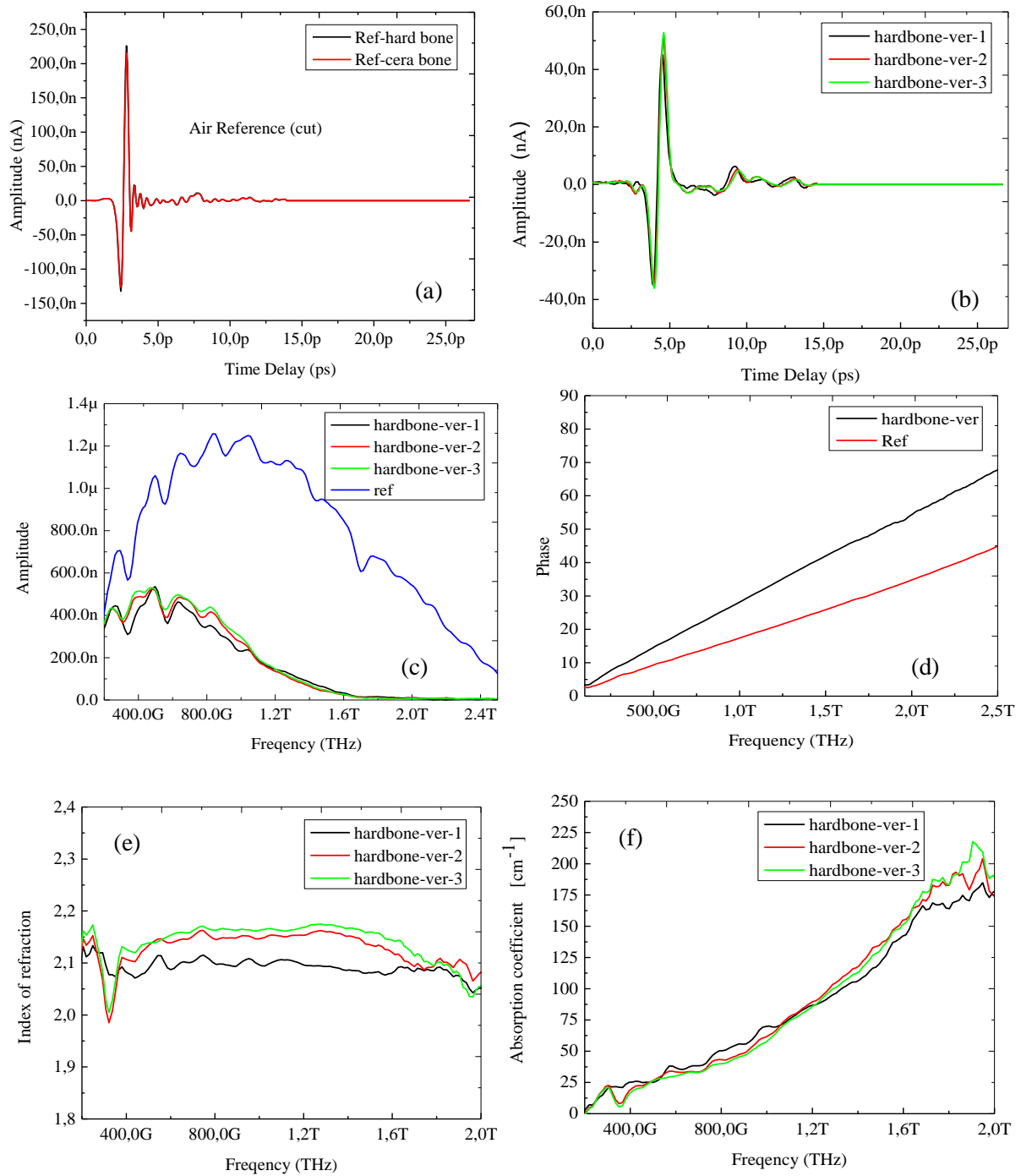


Figure 3. Temporal waveforms of THz pulses transmitted through (a) the air and (b) jawbone, THz amplitude spectra of the fields after a FFT (c); phase-frequency response (d); refractive index (e) and absorption coefficient human jawbone (f). The THz pulse polarization is parallel to the bone axis.

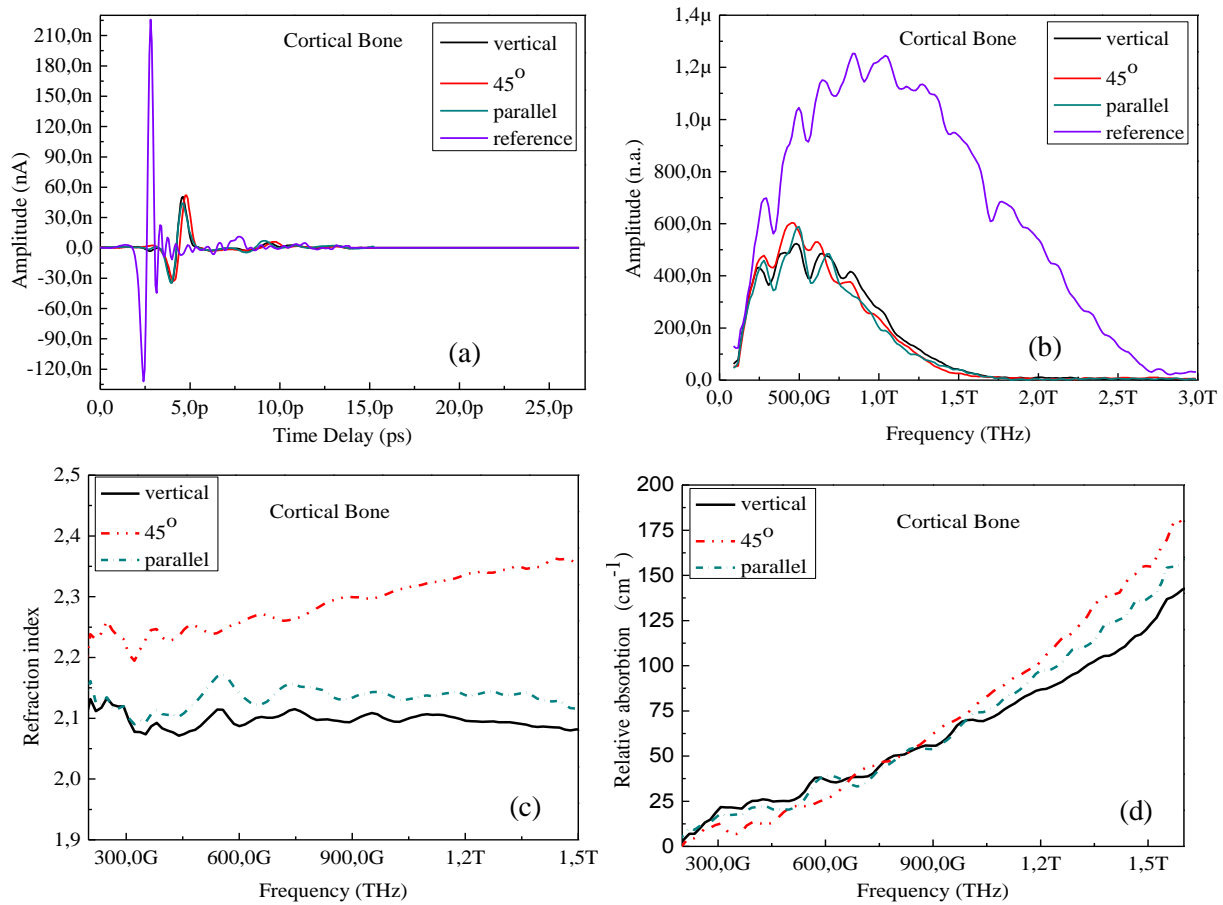


Figure 4. The index of refraction $n(f)$ and absorption coefficient $\alpha(f)$ for different directions of the THz polarization (vertical, 45° , and parallel to the bone axis), in the spectral range of 0.2-2.5 THz.

The difference between the absorption coefficient $\alpha(f)$ for different directions of the THz pulse polarization depend on the relationship between the sizes and the properties of the cylinders or plates, can take positive or negative values. For example, only at frequencies 250 GHz and 830 GHz the absorption coefficient $\alpha(f)$ for different directions of the THz pulse polarization is same, $\Delta\alpha = 0$, but at frequencies above 830 GHz $\Delta\alpha$ is positive, and below 830 GHz negative.

Table 1. Optical parameters $n(f)$ and $\alpha(f)$ of the jawbone depending on the orientation of the THz pulse polarization

Polarization	$n_{\max}(f)$	$n_{\min}(f)$	$\Delta n(f)$	$\alpha_{\min}(f), \text{cm}^{-1}$	$\alpha_{\max}(f)$	$\Delta\alpha(f)$
Horizontal	2.1725	2.0896	0.0829	7.132	157.514	150.38
Vertical	2.1332	2.0711	0.0621	3.956	142.200	138.24
45°	2.3631	2.1941	0.169	1.717	178.487	176.77

It is known that the variation amount of trace elements in bone causes osteomalacia, osteoporosis and other diseases. Crystals form mineralized bone varies from plate to the needle. In shape and size of the crystals can be affected by age, state of health. Throughout life, all bones are in a dynamic process of growth and resorption called reconstruction. Inhibition or lack of bone reconstruction accompanied by a deterioration of the mechanical properties and results in macro- and microfractures. All these factors can influence the anisotropy of the bone. The information about the tissue, obtained by THz pulses orthogonal polarizations will improve also the diagnosis of tissue - whether it is cancerous or not. Cancer cells produce large heterogeneity in healthy tissues in shape and chemical composition.

The use of orthogonally polarized pulses in THz imaging of tissues provides unprecedented potential for nondestructive mapping of anisotropy in tissues with cancer. It is well known that enlarged nuclei of the cell are primary indicators of cancer

Conclusions

Dielectric anisotropy of a human jawbone has been studied using THz time-domain transmission spectroscopy in the wide frequency range 0.2–2.5 THz in vitro. The refractive index $n(f)$ and absorption coefficient $\alpha(f)$ for different directions of the THz pulse polarization were measured. As the results of studies, it was found that the refractive index of the human jawbone changes between the values of 2.07 and 2.36 depending on the THz pulse polarization, and Cerabone® – between 2.4 and 2.65 [12]. The absorption coefficient of the human jawbone increases with the frequency from 1.7 cm^{-1} to a value of 178.5 cm^{-1} . The absorption coefficient of Cerabone® increases to 80 cm^{-1} , and the resonance absorption occurs at 1.7 THz [12]. The difference $n(\omega)$ and $\alpha(\omega)$ in different directions at any frequency can be associated with the structural anisotropy of a bone that is, both with different dimensions of the bone particles and a specific tissue structure.

It was found that before and after the 830 GHz $\Delta\alpha = \alpha_{\text{ver}} - \alpha_{\text{par}}$ and $\Delta\alpha = \alpha_{\text{ver}} - \alpha_{45^\circ}$ changes sign.

This is the first representation of the frequency-dependent refractive index $n(f)$ and absorption coefficient $\alpha(f)$ of human jawbone.

Acknowledgments

This research was supported by the National Instrumentation Program (Grant No.2012YQ140005), the National Nature Science Foundation of China (Grant Nos. 61505125), the Nature Science Foundation of Beijing (Grant No. 4144069) and Science and Technology Project of Beijing Municipal Education Commission (Grant No. KM201410028004).

References

- [1] Almany Magal R, Reznikov N, Shahar R, Weiner S 2014 Three-dimensional structure of minipig fibrolamellar bone: Adaptation to axial loading J. Struct. Biol. **186** 253–264
- [2] Berry E, Fitzgerald A J., Zinov'ev N N, Walker G C, Homer-Vanniasinkam S, Sudworth C D, Miles R E, Chamberlain J M, Smith MA 2003 Optical properties of tissue measured using Terahertz pulsed imaging Proceedings of SPIE: Medical Imaging: Physics of Medical Imaging **5030** 459-470
- [3] Tuchin V V 2015 Tissue Optics and Photonics: Biological Tissue Structures J. of Biomedical Photonics & Eng, **1** no.1 3-21

- [4] Reznikov N, Shahar R, Weiner S, 2014 *Acta Biomater* **10** 3815
- [5] Larry Arsenault A 1991 Image Analysis of Mineralized and Non-Mineralized Type I Collagen Fibrils. *J. of Electron Microscopy Technique* **18**, 262-268
- [6] Svetoslav Nikolov and Dierk Raabe Hierarchical June 2008 Modeling of the Elastic Properties of Bone at Submicron Scales: The Role of Extrafibrillar Mineralization. *Biophysical Journal* **94** 4220–4232
- [7] ErtsL D, Gathercole E J, Atkins D T 1994 Scanning probe microscopy of intrafibrillar crystallites in calcified collagen *J. of Materials Science: Materials in Medicine* **5** 200–206
- [8] Fitzgerald A J., Berry E, Zinov'ev N N, Homer-Vanniasinkam S, Miles RE, Chamberlain J M, and Smith M A, 2003 *J. Biol. Phys.* **29** 123.
- [9] Berry E, Fitzgerald A J, Zinov'ev N N, Walker G C, Homer-Vanniasinkam S, Sudworth C D, Miles R E, Chamberlain J M, and Smith M A, 2003 *Proceedings of SPIE*. **5030** 459
- [10] Zinov'ev N N, Nikoghosyan A S, and Chamberlain J M 2006 *Proceedings of SPIE*, **6257** 62570P1
- [11] Pickwell E, Wallace V P, Cole B E, Ali S, Longbottom C, Lynch R and Pepper M 2007 *Caries Res.*, **41** 4955.
- [12] Nikoghosyan A S, Ting H, Shen J, Martirosyan R M, Tunyan M Yu, Papikyan A V, Papikyan A A 2016 Optical properties of human jawbone and human bone substitute CERABONE® in the terahertz range *Journal of Contemporary Physics (Armenian Academy of Sciences)* **51** No. 3 256-264
- [13] A. Yariv 1983 *Introduction to Optical Electronics* Moscow, Высшая школа

Figure Caption

Figure 1. System of long dielectric cylinders array (mineralized collagen fibrils of turkey) with major components.

Figure 2. Experimental setup of THz spectrometer

Figure 3. Temporal waveforms of THz pulses transmitted through (a) the air and (b) jawbone, THz amplitude spectra of the fields after a FFT (c); phase-frequency response (d); refractive index (e) and absorption coefficient human jawbone (f). The THz pulse polarization is parallel to the bone axis.

Figure 4. The index of refraction $n(f)$ and absorption coefficient $\alpha(f)$ for different directions of the THz polarization (vertical, 45° , and parallel to the bone axis), in the spectral range of 0.2-2.5 THz.